

## PREDICTING WIND-DRIVEN WAVES IN SMALL RESERVOIRS

Y. Ozeren, D. G. Wren

**ABSTRACT.** *The earthen levees commonly used to form irrigation reservoirs are subjected to significant embankment erosion due to wind-generated waves. The design of bank protection measures relies on adequate prediction of wave characteristics based on wind conditions and fetch length. Current formulations are based primarily on winds and waves in large water bodies and do not provide an optimal fit to waves in small water bodies such as irrigation ponds. Based on wind and wave data collected in an irrigation reservoir near Carlisle, Arkansas, the coefficients in a commonly used equation for wind wave prediction were improved for use in irrigation reservoirs. Details of the development of the new coefficients as well as data collection procedures are presented here. With the new empirical coefficients, the RMS error is 0.01 m for energy-based significant wave height and 0.06 s for peak wave period.*

**Keywords.** *Erosion protection, Levee protection, Wave prediction, Wind measurement.*

Irrigation reservoirs are used to store water during winter months so that it can be used to irrigate crops during the growing season. Of the approximately 700 miles of earthen levees currently being used for irrigation ponds in the U.S., at least 50% experience significant damage due to wind-driven waves (Carman, 2003). Efforts to mitigate this damage require estimates of the size of waves that will impact the levees (Ozeren et al., 2008). Techniques developed for larger water bodies have been found to be inadequate for predicting wind-driven waves in irrigation reservoirs (Vincent et al., 2002).

The energy transferred to the water surface by wind generates a range of wave heights and periods that increase as the waves travel across the available fetch length. The process of wave generation by wind can be explained by combining the resonance model developed by Phillips (1957) and the shear flow model developed by Miles (1957). Pressure fluctuations within the wind field disturb the still water and cause water surface undulations. These pressure fluctuations moving in the direction of the wind resonate with the free wave speed and amplify the undulations. As the size of these undulations increases, they begin to affect the pressure distribution within the wind field, resulting in a pressure difference between two wave crests. The net force created by the higher pressure on the windward face of the wave results in wave growth. Another explanation for the energy transfer between wind and waves was developed by Longuet-Higgins (1969). As the wave heights increase, shorter waves steepen and break on the crests of faster traveling, longer waves. Therefore, as the speed, fetch, or

duration of the wind increases, wave height and period also increase.

If the wind blows with a constant speed and direction over a certain fetch for sufficient time for the waves to travel the entire fetch length, then the wave characteristics will only depend on the fetch length and wind speed. This is known as the fetch-limited condition, and it is assumed that steady-state wave conditions are achieved for that fetch (Vincent et al., 2002). If the wind duration is less than the required time for the waves to travel the fetch, then the wave conditions will be time dependent, and such wave conditions are described as duration-limited. The duration-limited condition is based on the assumption that wind speed increases suddenly in an area far from the boundaries, a condition that is rarely met. Wind blowing for an unlimited duration over an unlimited distance will have a limiting fetch length beyond which the waves do not continue to grow. This limiting condition is called a fully developed sea, and the rate of energy input to the waves from the wind is balanced with dissipation by wave breaking and turbulence (Sorensen, 1993).

Due to the complexity of the physical phenomena, most methods for wave prediction are based on semi-empirical relations. The methods have been modified as wind and wave data were accumulated over time, resulting in better predictions. The significant wave method (SMB method) was developed by Sverdrup and Munk (1947) and improved by Bretschneider (1952). The SMB method combines a simple energy growth concept with empirical calibrations using field data. Natural waves can be characterized by their frequency spectrum, which provides a measure of the energy at each frequency. Therefore, recent researchers seek to predict the wave energy spectrum given wind conditions (Sorensen, 1993). The simple empirical models of wave prediction assume uniform and steady wind conditions and neglect depth variations and shallow water processes. Discrete spectral and parametric methods of wave prediction have been developed to better represent the physical processes by coupling energy conservation principals with air-water and water-bed interaction processes. These models require numerical solution of complex equations with

---

Submitted for review in October 2008 as manuscript number SW 7755; approved for publication by the Soil & Water Division of ASABE in July 2009.

The authors are **Yavuz Ozeren**, Research Associate, Department of Biology, University of Mississippi, University, Mississippi; and **Daniel G. Wren**, Hydraulic Engineer, USDA-ARS National Sedimentation Laboratory, Oxford, Mississippi. **Corresponding author:** Daniel G. Wren, P.O. Box 1157, Oxford, MS 38655; phone: 662-232-2329; fax: 662-281-5706; e-mail: Daniel.Wren@ars.usda.gov.

empirical corrections that depend on the field conditions (Sobey, 1986).

There are several numerical models currently available for predicting wave fields under complex wind conditions and bathymetries. The third-generation spectral wave model (SWAN) was developed at the Technical University of Delft (Booij et al., 1999; Ris et al., 1999) and has been widely used in the coastal engineering and science community (Ding et al., 2006; Chen et al., 2007). The wave analysis model (WAM) was also developed as a global third-generation model to solve the balance equations based on the concept of a wind-wave energy spectrum (Komen et al., 1994; Lin et al., 2002). However, the current work is intended for use by field practitioners and will be confined to a relatively simple semi-empirical model for predicting wave characteristics based on wind conditions.

A parametric model to predict deepwater wave characteristics is recommended in the Shore Protection Manual (SPM, 1984). Vincent et al. (2002), in the Coastal Engineering Manual (U.S. Army Corps of Engineers, 2002), an updated version of the Shore Protection Manual, present a modified method for predicting wind-driven waves. Both the Shore Protection Manual (SPM, 1984) and Vincent et al. (2002) methods will be considered; however, due to its better performance for the current application, only the Shore Protection Manual (SPM, 1984) method will be modified for use in small reservoirs. New coefficients necessary for using the Shore Protection Manual (SPM, 1984) method in small reservoirs are calculated based on wind and wave characteristics measured in Schafer Lake, an irrigation pond near Carlisle, Arkansas. The results should be applicable to inland reservoirs of similar shape and size to Schafer Lake. There were no trees or surface relief other than the levee nearby, so the results given here can be generalized to other lakes. If vegetation or topography creates locally reduced

wind speeds in a subject lake, then the method given here can yield results that may serve as an upper limit for wave size.

## MATERIALS AND METHODS

### FIELD MEASUREMENTS

The first set of field measurements was collected on March 16, 2005, using a temporary wind and wave monitoring station in Schafer Lake. A photograph showing a typical arrangement for the instrumentation is given in figure 1. The reservoir is 770 m along the east/west axis and 370 m along the north/south axis. The prevalent wind direction for the day was observed to be from the northeast, so the measurement tower was positioned in the southwest corner of the reservoir (fig. 2). The water depth,  $h$ , at the installation point was 2.5 m. The embankments are constructed from soil pushed outward from the reservoir side, leaving deeper water near the banks. Based on the lack of relief in the surrounding area, bathymetric variations can be neglected far from the banks. Water level measurements were made using two ultrasonic distance sensors mounted approximately 35 cm from the mean water level. The ultrasonic distance sensors collected data at a rate of 10 Hz with  $\pm 1$  mm accuracy. Wind speed and direction were measured by a wind anemometer mounted 2 m above the mean water level on the same instrument platform used for the wave measurements. The accuracy of the wind speed sensor was 0.5 m/s in a range of 0 to 50 m/s.

A second set of field data was collected in April 2007 near the south shore of Schafer Lake (fig. 2). Here, capacitance level sensors were used to measure the water level at a rate of 30 Hz. The accuracy of the sensors within 20% to 80% of full length was 1.25 mm. Two wind speed and direction sensors were mounted on a separate tower at elevations 1.7 and 6 m above the mean water level. In May 2008, the

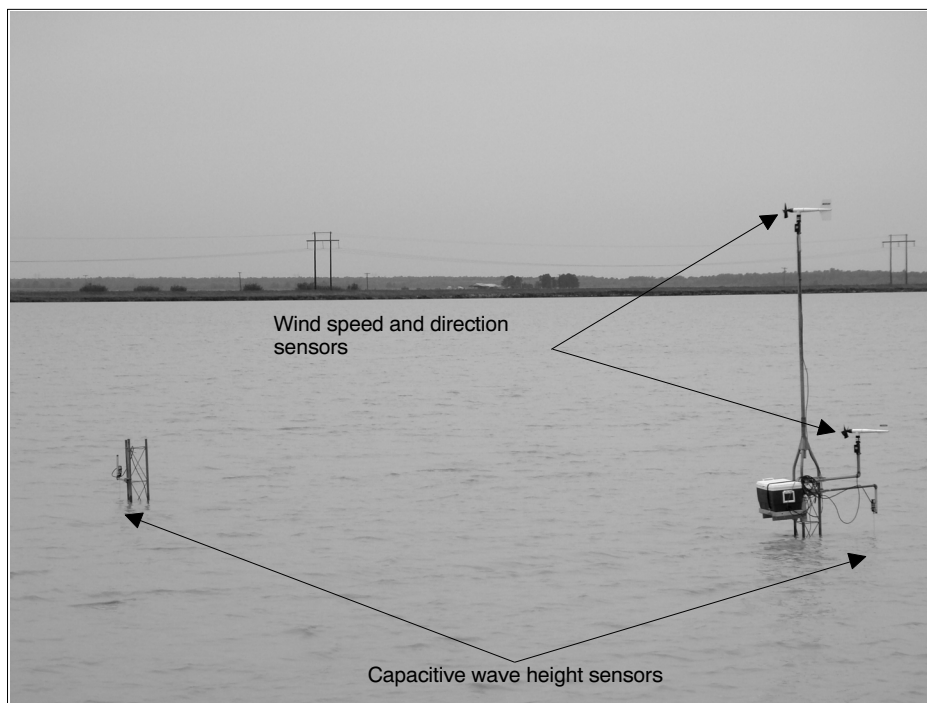


Figure 1. Field installation for wind and wave measurements.

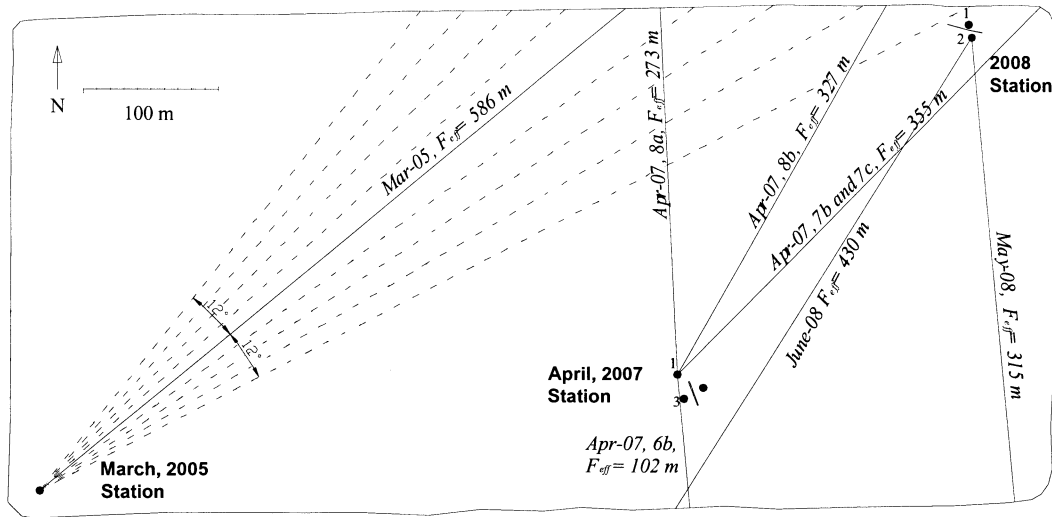


Figure 2. Layout of the measurement stations on Schafer Lake and corresponding fetch lengths.

measurement station was moved to the northeast corner of the reservoir (fig. 2). The same instruments were used as in the previous field work, and the wind sensors were 1.2 and 3.6 m above the mean water level. A final data set was collected in June 2008 with approximately 40 h of continuous wind-wave data from the same station as used in May 2008.

The time series of surface elevations was processed using spectral analysis. For each data set, the water surface elevation signal was divided into segments whose length depended on a minimum duration, which is defined below. Each of these segments was divided into 512 (51.2 s) point subsegments for spectral analysis. Both the main segments and subsegments were overlapped by 50%. Wave spectra within each segment were averaged for each frequency band to get the average spectrum along each interval. The parameters for each data set are summarized in table 1. The energy-based significant wave height,  $H_{mo}$ , is defined as four times the standard deviation of the water surface elevation data (Longuet-Higgins, 1969), and the standard deviation is calculated from the square root of the zeroth moment of the variance spectrum. The mean period,  $T_m$ , is approximated from the ratio of the zeroth and the first moments of the variance spectrum. Figures 3 and 4 show data collected in June 2008. More details on the instrument calibration, data collection, and results can be found in Ozeren et al. (2008) and Ozeren et al. (2009).

### SPM METHOD OF WAVE PREDICTION

The term SPM will be used from this point forward to refer to the Shore Protection Manual (SPM, 1984) and the wave

prediction method found there. In the SPM method, deepwater wave predictions are made using a parametric model based on the JONSWAP spectrum. The JONSWAP spectrum is a wave energy spectrum created for fetch-limited, deepwater conditions from a large number of marine wave data sets. The SPM method yields the energy-based significant wave height,  $H_{mo}$ , and peak period,  $T_p$ , based on wind speed, fetch, and duration, which can be expressed as:

$$H_{mo}, T_p = f(U_A, F, t_d, h) \quad (1)$$

where  $U_A$  is the wind stress factor,  $F$  is the fetch length,  $t_d$  is the wind duration, and  $h$  is the water depth. The wind stress factor accounts for the rate of momentum transfer from the wind into the waves, given by:

$$U_A = 0.71U_{10}^{1.23} \quad (2)$$

where  $U_{10}$  is the average wind speed at 10 m above the mean water level.

The SPM recommends the equivalent fetch to be calculated based on the narrow spread of energy in the wave spectrum. This procedure uses the mean of fetch lengths measured at  $3^\circ$  intervals over a range of  $12^\circ$  above and below the bearing of the average wind direction. Vincent et al. (2002) suggested that a straight-line fetch be used in calculations. The mean fetch defined in the SPM is used to account for the wind direction. This becomes important since wind at angles not normal to a shoreline will result in a range of possible fetch lengths. For example, for the field data

Table 1. Summary of collected data.

Data Set	Duration (min)	Wind Direction (deg. ccw from north)	Wind Speed, $U_{10}$ (mph)	Effective Fetch, $F$ (m)	Minimum Duration, $t_{min}$ (min)	Averaging Interval, $\Delta t$ (min)
March 2005	96	310 ±14	23 ±3	586	18	146
April 2007, 6b	50	182 ±12	10 ±0.6	102	7	9.1
April 2007, 7b	15	316 ±23	7 ±1.2	355	21	15.9
April 2007, 7c	63	3 ±11	7 ±0.6	355	16	15.9
April 2007, 8a	64	352 ±9	12 ±1.8	273	12	15.9
April 2007, 8b	90	327 ±6	14 ±1.3	327	14	15.9
May 2008	55	185 ±5	12 ±1	315	14	13.7
June 2008	2591 (43 h)	153 ±7	21 ±2	450	16	15.9

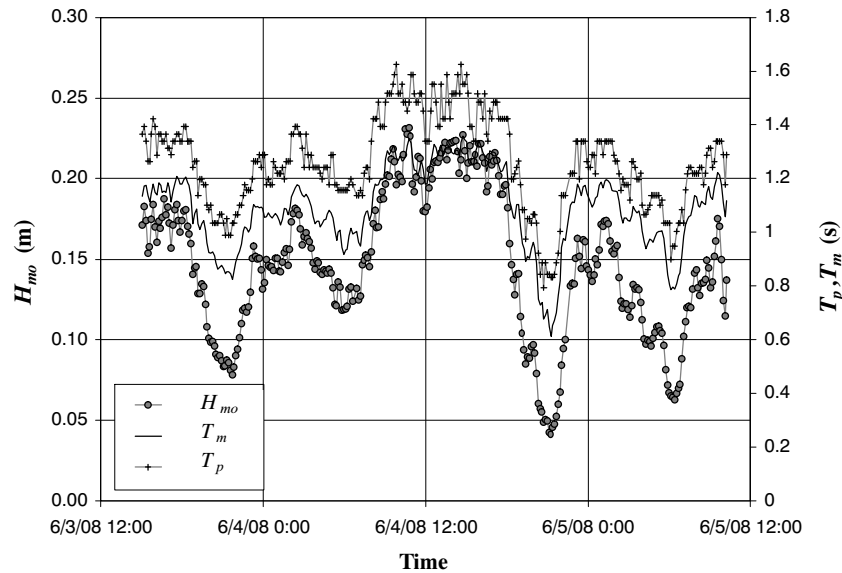


Figure 3. Energy-based significant wave height, mean period, and peak wave period for June 2008 data.

collected in the current study, a wide range of fetch lengths are within the  $\pm 12^\circ$  range. These data are better represented by the average fetch length than by the straight-line distance from the instruments to the shoreline in the direction of the prevailing wind.

Wave prediction requires knowledge of the wind velocity near the water surface over an appropriate averaging interval. Ideally, the time interval should be equal to the time needed for the waves to travel the available fetch and allow the assumption of fetch-limited conditions. The averaging interval was adjusted to make each data subset equal to the minimum wind duration required for the waves to travel the fetch length (table 1). For the March 2005 field data set, the power law given by equation 3a was used to estimate the wind speed at the 10 m elevation,  $U_{10}$ , using the measured wind speed values,  $U_z$ , at the  $z = 2$  m elevation:

$$U_{10} = U_z \left( \frac{10}{z} \right)^{1/7} \quad (3a)$$

For data from 2007 and 2008, wind speed at 10 m was estimated using data recorded at two different elevations and by assuming a logarithmic wind profile. The logarithmic wind profile is expressed by:

$$U_z = \frac{u_*}{k} \ln \left( \frac{z}{z_0} \right) \quad (3b)$$

where  $k$  is the von Kármán constant ( $k = 0.41$ ),  $z_0$  is the surface roughness height, and  $u_*$  is the shear velocity. The values of  $u_*$  and  $z_0$  are estimated by substituting the measured wind speed at two elevations into equation 3b. Then the wind

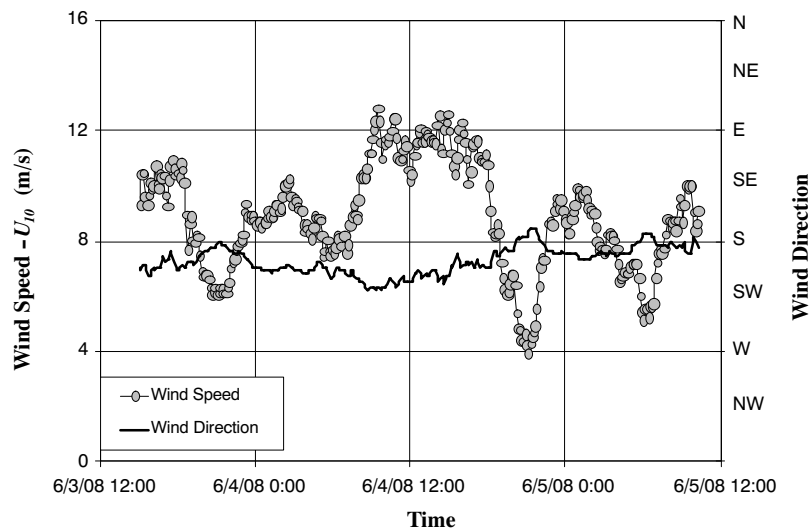


Figure 4. Wind speed at 10 m above the mean water level, and wind direction for June 2008 data. The letters on the right axis indicate the incoming wind direction.

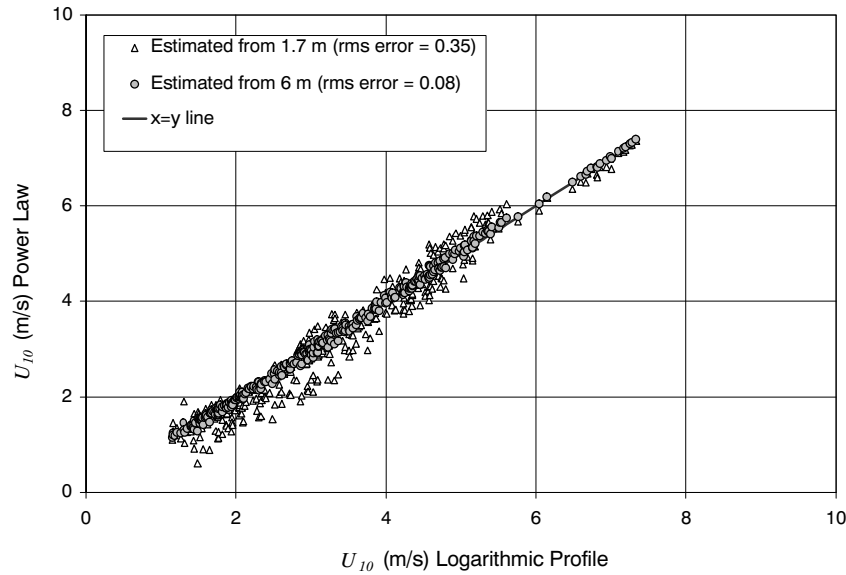


Figure 5. Comparison of wind speeds at 10 m extrapolated using the logarithmic wind profile and power law.

at 10 m is estimated by using the calculated values of  $u_*$  and  $z_0$ . The SPM suggests the use of equation 3a in an elevation range of 8 to 12 m. The data from 2007 were used to compare the estimated wind velocity at the 10 m elevation using equations 3a and 3b (fig. 5). As would be expected, the data recorded at 6 m provided a better estimation of  $U_{10}$  than the data recorded at 1.7 m. However, figure 5 shows that the use of the power law to estimate  $U_{10}$  based on the 2005 data set was valid.

Dimensional analysis of the basic wave generation relationship yields (Hughes, 1993):

$$\frac{gH_{mo}}{U_A^2}, \frac{gT_p}{U_A} = f\left(\frac{gF}{U_A^2}, \frac{gt_d}{U_A}, \frac{gh}{U_A^2}\right) \quad (4)$$

Waves are classified as deepwater waves if the depth is greater than half the wavelength (Dean and Dalrymple, 1991). Nearly all of the wave data collected by the authors in this study met the deepwater condition. Hence, the last term,  $(gh)/U_A^2$ , can be eliminated. The minimum duration,  $t_{min}$ , is the time required for waves to travel the fetch length. If the wind duration is less than  $t_{min}$ , then the waves are defined as duration-limited. After this duration has been exceeded, the waves are defined as fetch-limited. If the wind persists long enough in magnitude and direction for the waves to become fetch-limited, then the wave parameters no longer depend on  $(gt_d)/U_A$ . Equation 5 for the fetch-limited condition reduces to:

$$\frac{gH_{mo}}{U_A^2}, \frac{gT_p}{U_A} = f\left(\frac{gF}{U_A^2}\right) \quad (5)$$

The functional relationship in equation 5 states that  $H_{mo}$  and  $T_p$  are both a function of the fetch length and wind speed. The SPM (1984) gives the following parametric model for predicting deepwater waves from wind properties:

$$\frac{gH_{mo}}{U_A^2} = 0.0016\left(\frac{gF}{U_A^2}\right)^{1/2} \quad (6a)$$

$$\frac{gT_p}{U_A} = 0.286\left(\frac{gF}{U_A^2}\right)^{1/3} \quad (6b)$$

$$\frac{gt_{min}}{U_A} = 68.8\left(\frac{gF}{U_A^2}\right)^{2/3} \quad (6c)$$

Equation 6c is used for fetch-limited conditions, and the wind speed averaging interval was chosen to ensure that the fetch-limited condition was satisfied.

## RESULTS AND DISCUSSION

The relationships given in equations 6a through 6c are plotted for the data acquired in Schafer Lake in 2005, 2007, and 2008 in figures 6 and 7. The equations of the best fit lines are:

$$\frac{gH_{mo}}{U_A^2} = 0.0025\left(\frac{gF}{U_A^2}\right)^{0.44} \quad (7a)$$

$$\frac{gT_p}{U_A} = 0.4147\left(\frac{gF}{U_A^2}\right)^{0.28} \quad (7b)$$

In order to assume that the wave generation is fetch-limited, the wind must maintain a velocity for a sufficient time period. Since the wave train travels at group wave speed, the minimum duration for the waves to be fetch-limited can be approximated by integrating equation 7b over the fetch, which yields:

$$\frac{gt_{min}}{U_A} = 108.2\left(\frac{gF}{U_A^2}\right)^{0.28} \quad (8)$$

The wave parameters  $H_{mo}$  and  $T_p$  can be predicted for a given wind speed and direction using equations 2, 3, and 7.

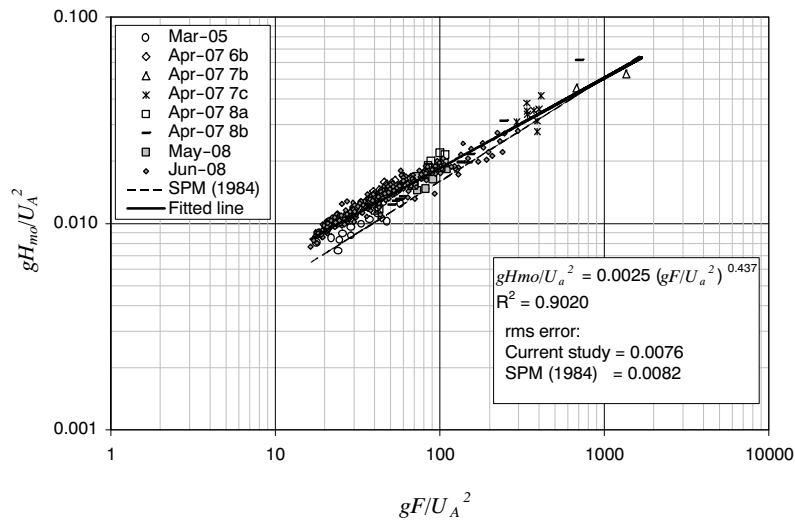


Figure 6. Wave prediction relationship for energy-based significant wave height estimates.

Figures 6 and 7 show that the model provides a good fit to the wave data, which cover a wide range of amplitude and period. The dashed lines in figures 6 and 7 were calculated using the SPM formulations given in equations 6a and 6b. The wave periods predicted by the SPM method in figure 6 were smaller than the measured values for the shorter wave periods. This may be due to reflected waves from the shore in the opposite direction of wave propagation. During the initial growth of the waves, energy is transferred from the high-frequency waves to lower frequencies, shifting the energy spectrum to a lower frequency range. Similarly, the measured wave heights are larger than those predicted with the SPM method for smaller waves.

In figure 8, measured values of  $H_{mo}$  and  $T_p$  are compared with the predicted values with the original SPM method, the Vincent et al. (2002) method, and the current approach. For the larger values of both  $H_{mo}$  and  $T_p$ , the current procedure gives better estimates than the SPM method. The low RMS values shown in figure 8 also indicate that the collected data

are consistent within the range of wind conditions given in table 1.

The shift in the energy density spectrum is illustrated in figure 9, where the average spectrum of a 6 h portion of the June 2008 data is compared with the JONSWAP spectrum for the same  $H_{mo}$  and  $T_p$ . The maximum time period of relatively constant wind speed and direction data from figure 3 (approx. 11:00 a.m. to 5:00 p.m. on June 4, 2008) was chosen for comparison with the JONSWAP spectrum. The shorter waves have more energy compared to the JONSWAP spectrum, and the total wave energy is larger than the predicted wave energy. The JONSWAP spectrum was expressed in terms of  $H_{mo}$  and  $T_p$  while holding the other parameters constant. Average values of the remaining parameters as found in the Coastal Engineering Manual (U.S. Army Corps of Engineers, 2002) were used.

A sample wave prediction is given below using the derived coefficients. Consider wind recorded at 8 m/s at an elevation of 3 m above the mean water surface at a location with 500 m fetch length and 2.5 m water depth:

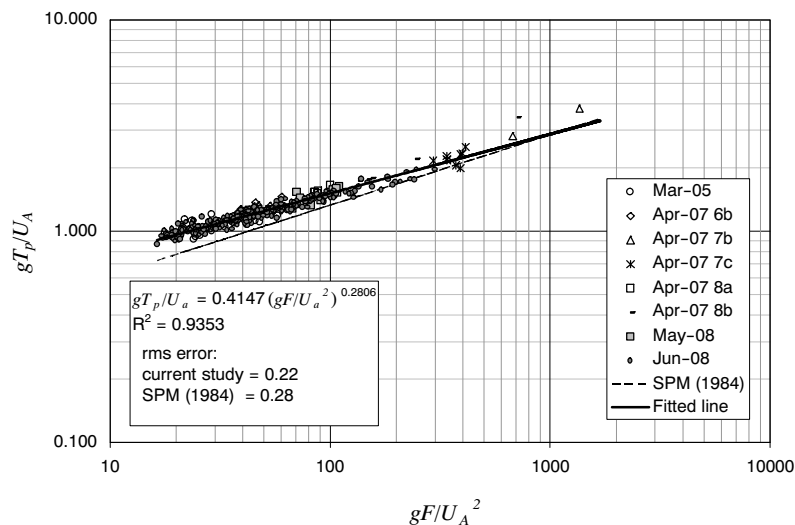


Figure 7. Wave prediction relationship for peak wave period estimations.

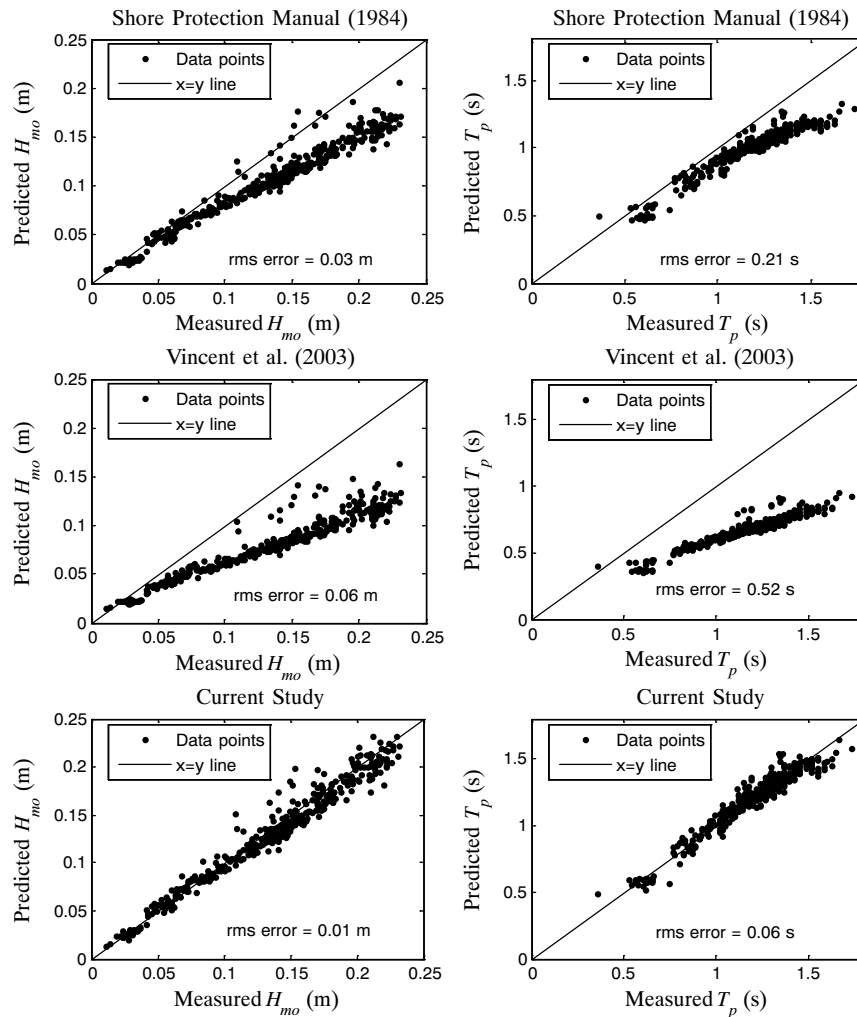


Figure 8. Comparison between SPM (1984) and Vincent et al. (2002) prediction of waves and prediction with coefficients determined in the current work.

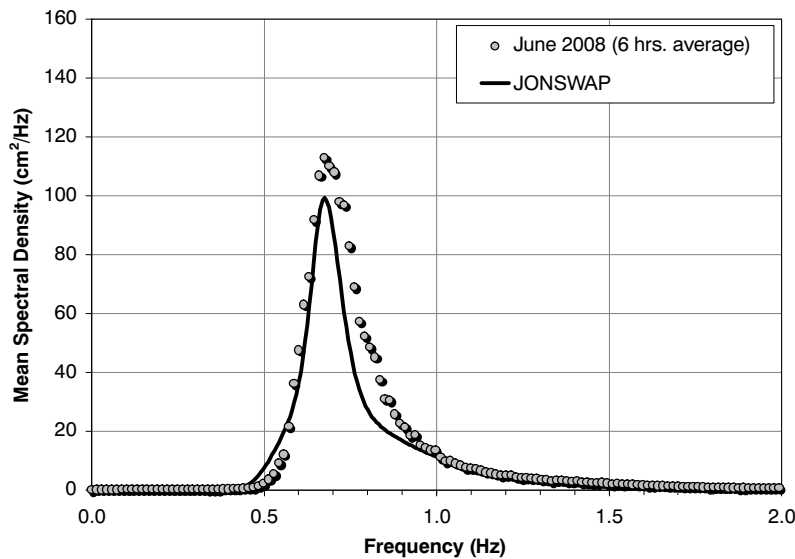


Figure 9. Comparison of the JONSWAP spectrum with 6 h of June 2008 data wave data.

1. Calculate wind speed,  $U_{10}$ , at 10 m (eq. 3a):

$$U_{10} = U_z \left( \frac{10}{z} \right)^{1/7} = 8 \cdot \left( \frac{10}{3} \right)^{1/7} = 9.5 \text{ m/s}$$

2. Calculate wind stress factor,  $U_A$  (eq. 2):

$$U_A = 0.71U_{10}^{1.23} = 0.71 \cdot 9.5^{1.23} = 11.3 \text{ m/s}$$

3. Calculate

$$\frac{gF}{U_A^2} = \frac{9.81 \cdot 500}{(11.3)^2} = 38.3$$

4. Check minimum duration (eq. 8):

$$\frac{gt_{\min}}{U_A} = 108.2 \left( \frac{gF}{U_A^2} \right)^{0.28}$$

$$t_{\min} = \frac{11.3 \cdot 108.2 \cdot 38.8^{0.28}}{9.81} = 347 \text{ s} = 5.8 \text{ min}$$

The wind speed is assumed to be constant during  $t_{\min}$ . Note that if the wind blows for a time less than  $t_{\min}$ , the fetch-limited assumptions will not be valid. In the SPM method, if the wave generation is duration-limited, a pseudo-fetch is calculated by replacing  $t_{\min}$  with  $t_d$  in equation 8, and wave parameters are recalculated using this pseudo-fetch.

5. Calculate  $T_p$  and  $H_{mo}$  (eqs. 7a and 7b):

$$\frac{gH_{mo}}{U_A^2} = 0.0025 \left( \frac{gF}{U_A^2} \right)^{0.44}$$

$$H_{mo} = \frac{0.0025 \cdot 38.8^{0.44} \cdot 11.3^2}{9.81} = 0.16 \text{ m and}$$

$$\frac{gT_p}{U_A} = 0.4147 \left( \frac{gF}{U_A^2} \right)^{0.28}$$

$$T_p = \frac{0.4147 \cdot 38.8^{0.28} \cdot 11.3}{9.81} = 1.33 \text{ s}$$

The accuracy of the wave prediction relies on the proper estimation of the wind field. The relationships presented here are based on the assumptions of uniform wind speed and deepwater conditions. Bathymetry effects can be significant, especially closer to the embankments. The confined nature of the irrigation pond introduces additional uncertainty due to the reflection of waves and wind field boundary-layer development. However, these same effects can also reduce uncertainty since the fetch length can be readily defined and waves are isolated from other effects. Another source of uncertainty is that the new coefficients rely on multiple data collection periods on a single reservoir.

## CONCLUSION

Wind and wave measurements collected in various conditions over a three-year period in an irrigation reservoir were used to improve the fit of the SPM method for predicting wind-driven waves based on wind characteristics and fetch length. The use of new coefficients provides an improved prediction for waves in small reservoirs. In contrast to previous formulations, the current approach was developed using data from a relatively small inland reservoir and resulted in better prediction for these conditions than those developed for coastal applications.

Although wave generation by wind is complex, it is possible to predict wave properties from the wind data at a steady-state when wind speed and direction data are available. Even though these data may not be available at a given field site, long-term estimates of wave characteristics should be valid if the prediction is based on wind data from the same region, as long as the topography near the weather station is similar to that of the irrigation reservoir. The flat topography of the land surrounding the reservoir combined with the lack of trees or other impediments to the wind should allow this data to be generalized to other areas. In locations where there is more shielding of the wind, the predictions found here will provide an estimate of the upper limits of expected wave size.

## ACKNOWLEDGEMENTS

The authors would like to thank Keith Admire at the USDA-NRCS National Water Management Office in Little Rock, Arkansas, for supporting this work. While there, Dennis Carman initiated the work and has continued to be a valuable resource. M. Altinakar is also recognized for his helpful comments and criticism. Glenn Gray provided invaluable technical support for all phases of the work.

## REFERENCES

- Booij, N., R. C. Ris, and L. H. Holthuijsen. 1999. A third-generation wave model for coastal regions: Part 1. Model description and validation. *J. Geophysical Res.* 104(C4): 7649-7666.
- Bretschneider, C. L. 1952. The generation and decay of wind waves in deep water. *Trans. American Geophysical Union* 33: 381-389.
- Carman, D. 2003. Personal communication with Dennis Carman, P.E., Chief Engineer and Director, White River Irrigation District, Stuttgart, Arkansas, 12 August 2003.
- Chen, Q., L. Wang, H. Zhao, and S. L. Dougless. 2007. Prediction of storm surges and wind waves on coastal highways in hurricane-prone areas. *J. Coastal Res.* 23(5): 1304-1317.
- Dean, G. D., and R. A. Dalrymple. 1991. *Water Wave Mechanics for Engineers and Scientists*. Hackensack, N.J.: World Scientific.
- Ding, Y., S. S. Y. Wang, and Y. Jia. 2006. Development and validation of a quasi three-dimensional coastal area morphological model. *J. Waterway, Port, Coastal, and Ocean Eng.* ASCE 132(6): 462-476.
- Hughes, S. A. 1993. *Physical Models and Laboratory Techniques in Coastal Engineering*. Hackensack, N.J.: World Scientific.
- Komen G. J., L. Cavaleri, M. Donelan, K. Hasselmann, S. Hasselmann, and P. A. E. M. Janssen, eds. 1994. *Dynamics and Modeling of Ocean Waves*. Cambridge, U.K.: Cambridge University Press.
- Lin, P. C., D. J. Schwab, and R. E. Jensen. 2002. Has wind-wave modeling reached its limits? *Ocean Eng.* 29(1): 81-98.
- Longuet-Higgins, M. S. 1969. A non-linear mechanism for the generation of sea waves. *Proc. Royal Soc. London A* 311(1506): 371-389.
- Miles J. W. 1957. On the generation of surface waves by shear flows. *J. Fluid Mech.* 3: 185-204.
- Ozeren, Y., D. G. Wren, and C. V. Alonso. 2008. Development of floating wave barriers for cost-effective protection of irrigation and catfish pond levees. *Trans. ASABE* 51(5): 1599-1612.
- Ozeren, Y., D. G. Wren, and C. V. Alonso. 2009. Experimental and Numerical Investigations of Floating Breakwater Performance. National Sedimentation Laboratory Technical Report #65.
- Phillips, O. M. 1957. On the generation of waves by turbulent winds. *J. Fluid Mech.* 2: 417-445.

- Ris, R. C., L. H. Holthuijsen, and N. Booij. 1999. A third-generation wave model for coastal regions: Part 2. Model description and validation. *J. Geophysical Res.* 104(C4): 7667-7681.
- Sobey R. 1986. Wind wave prediction. *Annual Rev. Fluid Mech.* 18: 149-172.
- Sorensen, R. M. 1993. *Basic Wave Mechanics for Coastal and Ocean Engineers*. New York, N.Y.: John Wiley and Sons.
- SPM. 1984. *Shore Protection Manual*. Vol. 2, 4th ed. Washington, D.C.: U.S. Army Engineer Waterways Experiment Station.
- Sverdrup, H. U., and W. H. Munk. 1947. Wind sea and swell: Theory of relations for forecasting. Publication 601. Washington, D.C.: U.S. Navy Hydrographic Office.
- U.S. Army Corps of Engineers. 2002. *Coastal Engineering Manual*. Engineer Manual 1110-2-1100 (6 volumes). Washington, D.C.: U.S. Army Corps of Engineers.
- Vincent, C. L., Z. Demirebilek, and J. R. Weggel. 2002. Chapter II-3. Estimation of nearshore waves. In *Coastal Engineering Manual: Part II. Coastal Hydrodynamics*. Engineer Manual 1110-2-1100. L. Vincent and Z. Demirebilek, eds. Washington, D.C.: U.S. Army Corps of Engineers.

